Int. J. Heat Mass Transfer. Vol. 1, pp. 173–191. Pergamon Press 1960. Printed in Great Britain.

ANALYSIS OF THE FLOW AND ENERGY SEPARATION IN A TURBULENT VORTEX

R. G. DEISSLER and M. PERLMUTTER
Lewis Research Center, National Aeronautics and Space Administration,
Cleveland, Ohio

(*Received* 16 *June* 1959)

Abstract—An analysis is made of the velocity, temperature and pressure distributions in a turbulent vortex with radial and axial flow. For making the calculations the vortex is divided into a core and an annular region, each with a different uniform axial mass velocity, although the equations obtained are applicable to an arbitrary axial mass velocity distribution. Tangential velocity, temperature and pressure distributions, as well as curves for overall energy or temperature separation, are presented and compared with experiment.

Using the analytical results, the causes of the energy separation are studied. It is concluded that the most important factor affecting the total temperature of a fluid element in a compressible vortex is the turbulent shear work done on or by the element.

Résumé—Une analyse est faite des distributions de vitesses, de températures et de pressions dans un tourbillon turbulent à écoulement radial et axial. Pour faire les calculs, le tourbillon a été divisé en deux régions: noyau et région annulaire, chaque région possédant une vitesse axiale uniforme différente, bien que les équations obtenues soient applicables à une distribution arbitraire des vitesses axiales. Les distributions de vitesses tangentielles, de températures et de pressions, ainsi que des courbes pour la séparation d'énergie et de température de l'ensemble, sont présentées et comparées à l'expérience.

Les causes de la séparation d'énergie sont étudiées à partir des résultats analytiques. En conclusion, le facteur le plus important affectant la température totale d'un élément de fluide dans un tourbillon compressible est le travail de cisaillement turbulent effectué sur, ou par, l'élément.

Zusammenfassung—Die Verteilungen der Geschwindigkeit, der Temperatur und des Drucks in einem turbulenten Wirbel wurden für radialen und axialen Strom untersucht. Hierzu wurde der Wirbel in einen Kern und einer Ringzone eingeteilt, wobei für jede eine verschiedene, aber einheitliche axiale Massengeschwindigkeit angenommen wurde, obwohl die erhaltenen Gleichungen auch für eine beliebige Verteilung der axialen Massengeschwindigkeit gelten. Die Verteilungen der Tangentialgeschwindigkeit, der Temperatur und des Druckes wurden ebenso wie die Kurven für die Trennung der Gesamtenergie oder der Temperatur angegeben und mit dem Experiment verglichen.

Unter Benutzung dieser Rechenergebnisse wurden die Ursachen für die Energietrennung untersucht. Es wird geschlossen, daß der wichtigste Faktor, der die Gesamttemperatur eines Flüssigkeitselementes in einem kompressiblen Wirbel beeinflußt, die turbulente Scherarbeit ist, die an einem oder durch ein Element geleistet wird.

Abstract—Основной задачей настоящей работы является исследование распределения скорости, температуры и давления в турбулентном вихре. В основе анализа положено схематическое представление о разделении вихря на ядро и наружную область. Каждая область имеет свою собственную постоянную скорость перемещения массы вдоль оси, хотя полученные уравнения можно применить для случая произвольного распределения скорости и движения массы по осям. Получены графики распределения температуры, давления, потенциальной скорости, а так же поля температуры и энергии, которые сопоставлены с экспериментальными данными. На основе аналитического исследования авторы пришли к заключению, что наиболее важным фактором, влияющим на полную локальную температуру газо-жидкостного сжимаемого вихря, является работа турбулентного перемещения.

NOMENCLATURE

c_p, specific heat;
$\frac{D}{D\theta}$, substantial derivative; $u \frac{d}{dr}$ as used here;
K, parameter $\left[W_h\left(\frac{r_0}{r_i}\right)^2 - 1\right] \Big/ W_c$;
k, thermal conductivity;
M_0 Mach number based on tangential velocity at outer radius;
P, stagnation or total pressure;
p, static pressure;
Re_i, Reynolds number, $-u_i r_i \rho_i / \rho\varepsilon$;
Re_0 Reynolds number based on outer radius; $Re_i\ W/W_c$;
r', nondimensional distance along radial co-ordinate, r/r_i;
T, t, total and static temperatures;
T', t', nondimensional total and static temperature, $T/(v_i^2/2c_p)$, $t/v_i^2/2c_p$;
T_c, mean total temperature of fluid leaving core;
T_e, mean total temperature of fluid entering vortex tube;
T_h, mean total temperature of fluid leaving annulus;
u, v, w, radial, angular and axial components of velocity;
W, total mass flow entering system;
W_c, mass flow leaving core;
W_h, mass flow leaving annulus;
v', nondimensional angular velocity, v/v_i;
z, distance along axial co-ordinate;
γ, ratio of specific heats;
ε, eddy diffusivity;
θ, time;
θ', dimensionless time; $-(u_i/r_i)\theta$;
μ, viscosity;
ρ, density;
τ, turbulent shear stress, $\rho\varepsilon(dv/dr - v/r)$;
τ', dimensionless turbulent shear stress $\frac{1}{Re_i}\left(\frac{dv'}{dr'} - \frac{v'}{r'}\right)$;
ϕ, turbulent dissipation $= \rho\varepsilon(dv/dr - v/r)^2$;
ϕ', dimensionless turbulent dissipation; $\frac{2}{Re_i}\left(\frac{dv'}{dr'} - \frac{v'}{r'}\right)^2$.

Subscripts
i, pertaining to core or reference radius;
0, pertaining to outer radius of vortex.

INTRODUCTION

THE problem considered here is that of the velocity and temperature distributions in a turbulent compressible vortex with radial and axial flow. That problem occurs, for instance, in connection with the Ranque–Hilsch vortex tube [1]. In that apparatus gas enters a tube tangentially through nozzles so as to form a vortex within the tube. Cold gas can then be withdrawn axially from the region near the center of the tube and hot gas from the annular region at larger radii. A total temperature or energy separation thus occurs within the vortex. The vortex tube should be useful for obtaining quantities of either hot or cold air. The feature of no moving parts might make it especially attractive for applications where extreme temperatures are desired. For instance, a vortex tube might conceivably be used to obtain higher propellant temperatures in a nuclear rocket than could be obtained by the nuclear reactor alone, which is limited in temperature by the reactor materials. The walls of the vortex tube could be cooled to prevent melting, and the cold stream from the vortex could be reheated in the reactor.

A great deal of work, both experimental and analytical, has been done in connection with the phenomenon described above. A summary of the work done between 1931 and 1953 is given in [2]. Some additional investigations since that time are given in [3, 7, 12]. Although many of the important factors in the phenomenon have been considered in one or another of the previous papers, it appears that all of the analyses neglected at least some of the important factors. Also, a more thorough discussion of the causes of the energy separation would be desirable. The present writers in a preliminary study [5], of which the present paper is a refinement and extension, have attempted to include the pertinent terms in the compressible laminar and turbulent momentum and energy equations. Only the turbulent case is considered herein. inasmuch as it was shown in [5] that the energy separation in actual vortex tubes cannot be accounted for by considering a laminar vortex.

(Energy separation can also occur in a laminar vortex but the radial flow must be extremely small.) The effect of energy diffusion due to the expansion and contraction of the turbulent eddies as they move radially in a pressure gradient is included in the equations.

The model considered (Fig. 1) is an axially symmetric vortex in which the tangential velocity and temperature are independent of axial position. The tangential and radial velocities, as well as the temperature, are specified at a reference radius. In addition, the axial mass

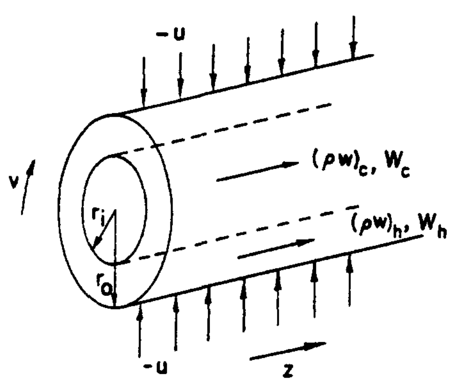

FIG. 1. Vortex model used in analysis.

velocity is specified as a function of radius and axial position. As will be shown, only a linear variation of axial mass velocity with axial position is consistent with the assumption of a tangential velocity independent of axial position, but the variation of axial velocity with radius can be arbitrary. For the present calculations a uniform axial mass velocity $(\rho w)_c$ in a region near the center and a different uniform axial velocity $(\rho w)_h$ in the remaining annular region were assumed. The analysis predicts the tangential velocity and temperature as functions of radius. For calculating the temperature distributions it was assumed, in order to make the equations tractable, that squares of axial and radial velocities are small compared with squares of the tangential velocities.

VELOCITY DISTRIBUTIONS

In the present model the flow is taken to be axially symmetric and steady state with no body forces. For that case the compressible Navier–Stokes equation for the tangential component of the velocity [8], reduces to

$$\rho u \frac{\partial v}{\partial r} + \rho w \frac{\partial v}{\partial z} + \frac{\rho u v}{r} = \frac{\partial}{\partial z}\left(\mu \frac{\partial v}{\partial z}\right) + \frac{\partial}{\partial r}\left\{\mu\left(\frac{\partial v}{\partial r} - \frac{v}{r}\right)\right\} + \frac{2\mu}{r}\left(\frac{\partial v}{\partial r} - \frac{v}{r}\right) \quad (1)$$

For turbulent flow the increased shear stress due to the turbulence can be accounted for by replacing μ by $\mu + \rho\varepsilon$ in the momentum equation. The quantity $\rho\varepsilon$ is the eddy viscosity and depends on the turbulent mixing at a point. Except near boundaries, or at low Reynolds numbers, μ is small compared to $\rho\varepsilon$ and can be neglected. Although $\rho\varepsilon$ is in general a variable, it appears reasonable to assume that it can be considered constant for a vortex with radial flow. This assumption is in agreement with the experiments in [6] for incompressible flow. Because of lack of information on compressible vortex flow, and because of the considerable simplification obtained, we will assume that $\rho\varepsilon$ can be considered constant also for compressible flow and then attempt to justify the assumption by comparison of the results with experiment.

Inasmuch as our model assumes that v is independent of z, equation (1) becomes, for turbulent flow:

$$\rho u \frac{dv}{dr} + \frac{\rho u v}{r} = \rho\varepsilon\left(\frac{d^2 v}{dr^2} + \frac{1}{r}\frac{dv}{dr} - \frac{v}{r^2}\right) \quad (2)$$

Essentially the same result could have been obtained by dividing the instantaneous velocities and densities in equation (1) into mean and fluctuating components, taking time averages, and setting the Reynolds stress

$$\overline{u'v'} = -\varepsilon(dv/dr - v/r)$$

by analogy with the laminar shear stress. Note from equation (2) that the assumption that v is independent of z implies that ρu is also independent of z. The general solution of equation (2) is:

$$v = \frac{c_1}{r}\int r \exp\left(\int \frac{\rho u}{\rho\varepsilon}\, dr\right) dr + \frac{c_2}{r} \quad (3)$$

Using the boundary condition that the velocities at the axis of the vortex cannot be infinite, equation (3) can be written in dimensionless form as

$$v' = \frac{\int_0^{r'} r' \exp\left(\int_0^{r'} \frac{\rho u r_i}{\rho \varepsilon}\, dr'\right) dr'}{r' \int_0^1 r' \exp\left(\int_0^{r'} \frac{\rho u r_i}{\rho \varepsilon}\, dr'\right) dr'} \tag{4}$$

where the subscript i refers to values at a reference radius and the primes indicate that the quantities have been divided by their values at r_i.

In order to relate the radial flow to the axial flow, we use the continuity relation

$$\frac{\partial (r\rho u)}{\partial r} + \frac{\partial (r\rho w)}{\partial z} = 0 \tag{5}$$

Integrating equation (5) between the axis and the radius r results in

$$r\rho u = -\int_0^r \frac{\partial(\rho w)}{\partial z}\, r\, dr \tag{6}$$

Inasmuch as ρu is a function only of r, equation (6) shows that $\partial(\rho w)/\partial z$ is a function only of r. Therefore

$$\rho w = [\rho w(r)]_0 + f(r) z \tag{7}$$

where the subscript zero refers to values at $z = 0$.

In order to make numerical calculations it is necessary to assume a variation of $\partial(\rho w)/\partial z$ or of ρw with r. The vortex is divided into two regions, a core with radius r_i, and an annular region with inner and outer radii r_i and r_0 (Fig. 1). In each of these regions ρw, and thus $\partial(\rho w)/\partial z$ (equation (7)), is assumed independent of r, but there can be a step change in ρw at the interface between the two regions. Note that it is not necessary for the axial flow to be in the positive direction in both regions.

Consider first the core region. Dividing equation (6) by the same equation evaluated at r_i, and integrating, show that

$$\rho u/\rho_i u_i = r/r_i \tag{8}$$

Equation (4) then becomes

$$v' = \frac{1}{r'}\left(\frac{1 - \exp(-Re_i r'^2/2)}{1 - \exp(-Re_i/2)}\right) \tag{9}$$

where

$$Re_i = -\frac{\rho_i u_i r_i}{\rho \varepsilon}$$

The negative sign is included in the definition of Reynolds number because u_i is negative in the cases of interest here. Equation (9) was obtained by Einstein and Li [6]. For very large radial flows, equation (9) reduces to $v' = 1/r'$ (inviscid flow) except close to the center, whereas for small radial flows, $v' = r'$ (wheel flow).

For calculating velocities in the annulus, with ρw independent of r, one can break the integral in equation (6) into two parts, one with limits 0 and r_i, the other with limits r_i and r. Dividing the equation by $r_i \rho_i u_i$, integrating and making use of equation (7), result in

$$\frac{r\rho u}{r_i \rho_i u_i} = 1 + K(r'^2 - 1) \tag{10}$$

where

$$K = \frac{W_h/W_c}{(r_0/r_i)^2 - 1} \tag{11}$$

and W_h and W_c are the total axial flow out of the annulus and the core, respectively. Breaking the integrals in the numerator of equation (4) into two parts, substituting equations (8) and (10), and carrying out the integrations, result in the following equation for v' for the annulus.

$$v' = \frac{Re_i \exp(Re_i K/2)}{\exp(Re_i/2) - 1} \frac{1}{r'} \int_1^{r'} r'^{\,Re_i(K-1)+1} \times \exp(-Re_i K r'^2/2)\, dr' + \frac{1}{r'} \tag{12}$$

Equations (9) and (12) automatically satisfy the condition that dv'/dr' is continuous at $r' = 1$. Equation (12) can be integrated numerically.

Typical predicted tangential velocity distributions for several values of turbulent Reynolds number and of axial mass-flow ratio are presented in Fig. 2. In these curves Re_0 rather than Re_i is used as a parameter, where

$$Re_0 \equiv \rho_0 u_0 r_0/\rho\varepsilon = Re_i\, W/W_c$$

W is the total flow out of both the core region and the annulus. (A possible method for predicting the turbulent Reynolds number will be discussed in the next section.) These curves were calculated for a radius ratio r_0/r_i of 2·2. Other radius ratios give similar results, but the peaks of the curves fall closer to the center of the vortex

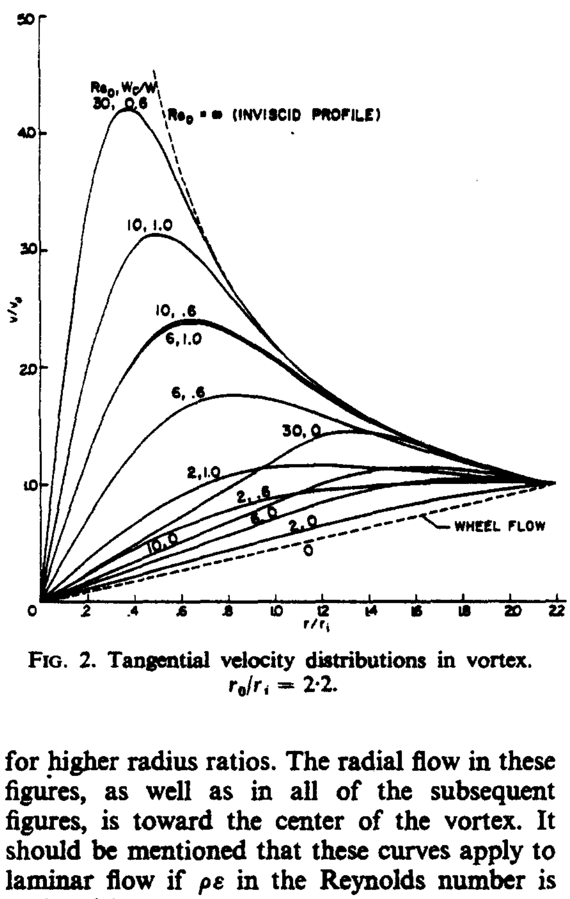

FIG. 2. Tangential velocity distributions in vortex. $r_0/r_i = 2{\cdot}2$.

for higher radius ratios. The radial flow in these figures, as well as in all of the subsequent figures, is toward the center of the vortex. It should be mentioned that these curves apply to laminar flow if $\rho\varepsilon$ in the Reynolds number is replaced by μ.

The curves for large values of W_c/W and small Reynolds number behave similarly to those for large values of Reynolds number and small W_c/W. The limiting curve for a radial flow Reynolds number of zero corresponds to wheel flow, whereas the curve for $Re_0 = \infty$ corresponds to inviscid vortex flow. Except at the lower Reynolds numbers the curves tend to approach the inviscid flow line ($v/v_0 = r_0/r$) in the outer region, whereas they approach wheel flow near the center. That is, it appears that the flow in the outer region is governed by inertia effects, whereas near the center the viscous effects become more important. This can be seen more clearly if we write the momentum equation (equation (2)) in the following form:

$$\frac{\rho}{\rho_i}\frac{Dv'}{D\theta'} = \frac{\rho u}{\rho_i u_i}\frac{v'}{r'} + \left(\frac{d\tau'}{dr'} + \frac{2\tau'}{r'}\right) \qquad (13)$$

where $\theta' \equiv -u_i\theta/r_i$ is a dimensionless time,

$$\tau' \equiv (dv'/dr' - v'/r')/Re_i \qquad (14)$$

is a dimensionless shear stress, and Re_i is the radial flow Reynolds number evaluated at some reference radius. The terms on the right side of this equation give the contributions which go to increase or decrease the tangential velocity of a particle at a given radius, as it moves toward the center of the vortex. The first term on the right side represents an inertia force per unit volume and tends to accelerate the particle in order to maintain constant angular momentum. The second term represents the net viscous shear force acting on the particle and tends to slow it down. These terms, together with the term on the left side of the equation giving the net rate of change of velocity of the particle, are plotted in Fig. 3 for the case where the axial velocity is uniform throughout the vortex. This case is shown for illustrative purposes; other axial velocity distributions should give qualitatively similar results. It is seen that in the outer regions (or for high Reynolds numbers) the net viscous force tending to slow the particle down is negligible compared with the inertia effect, so that constant angular momentum is preserved in that region. (Note that the curve for the inertia term also represents the tangential velocity profile in this particular case.) The fact that the net viscous shear force on the element is negligible means only that the tangential shearing forces on the sides of the element cancel, although they may be individually appreciable. In the region closer to the center (or for lower Reynolds numbers) the inertia and viscous forces become of the same order of magnitude, and at the center the ratio of viscous to inertia terms approaches 2. Thus the fluid particle decelerates in that region. Inasmuch as the radial velocity goes to zero at the center, one might have expected the ratio of viscous to inertia terms to approach infinity rather than 2 at that point. However, it should be pointed out that the viscous stress exists only because of the inertia effect; for wheel flow there would be no viscous stress. It is the deviation from wheel flow produced by the inertia effect which gives rise to the viscous shear stress.

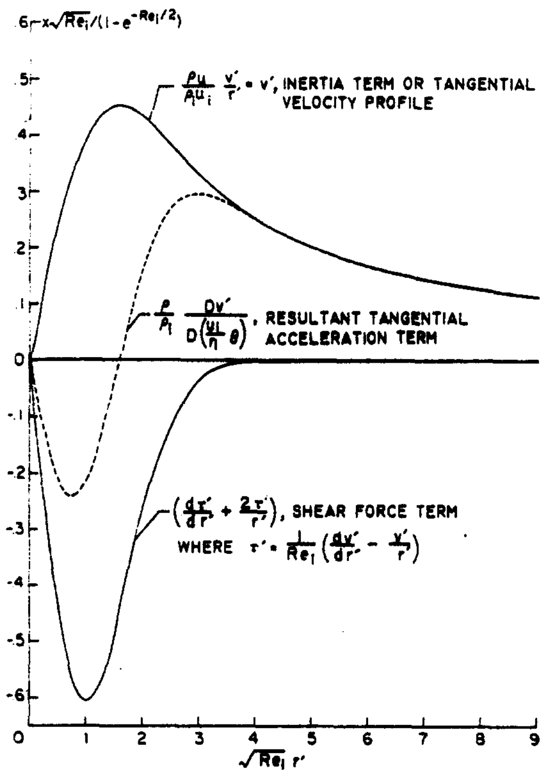

FIG. 3. Terms in momentum equation (equation (13)) contributing to local rate of change of velocity of fluid element with respect to time. Uniform axial mass velocity.

In order to determine whether the analytical method gives velocity distributions in reasonable agreement with experiment, the data of Hartnett and Eckert [7] were used. Those investigators measured velocity and temperature distributions at various axial positions in a vortex tube. Most of the axial flow occurred in the outer regions of the vortex, inasmuch as there was no opening at the vortex center. Although the axial mass velocity was not uniform in the outer region, it was assumed for purposes of comparison with the analysis, that the vortex could be divided into an outer region with uniform axial mass velocity, and an inner core, where the axial velocity is zero. It would have been possible to work out the analysis using the experimental axial velocity distributions, but the above simpler procedure was adopted. The data closest to the inlet nozzle are compared with analytical results for $W_c/W = 0$ in Fig. 4. For calculating the analytical curves, it was estimated from the data that

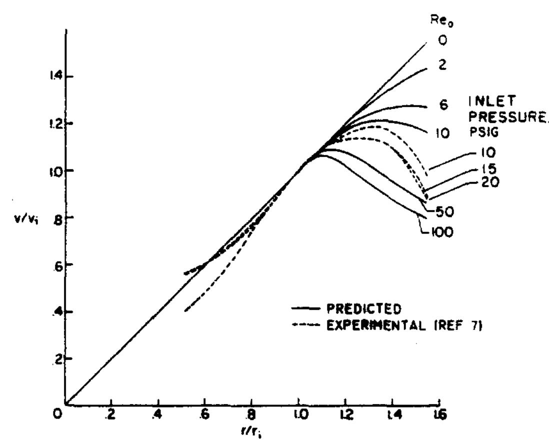

FIG. 4. Comparison of analytical tangential velocity profiles with experiments in [7]. $W_c/W = 0$, $r_0/r_i = 1{\cdot}54$.

the radius ratio for the outer and inner regions is about 1·54. This value gives approximately no net axial flow in the core for the experimental data. The shapes of the analytical and experimental curves agree reasonably well, indicating that the turbulent radial flow Reynolds numbers Re_0 lie between 10 and 50. These values are probably too high, however, because the effect of viscosity tends to make the velocities low near the tube wall. Viscous boundary layer effects are, of course, neglected in the analysis.

TEMPERATURE AND PRESSURE DISTRIBUTIONS

The steady-state energy equation for the compressible, axially symmetric flow of a perfect gas is [8]

$$\left.\begin{aligned}\rho c_p\left(u\frac{\partial t}{\partial r}+w\frac{\partial t}{\partial z}\right)-u\frac{\partial p}{\partial r}-w\frac{\partial p}{\partial z}&=\\ =\frac{1}{r}\frac{\partial}{\partial r}\left(rk\frac{\partial t}{\partial r}\right)+\frac{\partial}{\partial z}\left(k\frac{\partial t}{\partial z}\right)&+\\ +\mu\left[2\left\{\left(\frac{\partial u}{\partial r}\right)^2+\left(\frac{u}{r}\right)^2+\left(\frac{\partial w}{\partial z}\right)^2\right\}\right.&+\\ \left.+\left(\frac{\partial u}{\partial z}+\frac{\partial w}{\partial r}\right)^2+\left(\frac{\partial v}{\partial r}-\frac{v}{r}\right)^2\right]&-\\ -\frac{2\mu}{3}\left(\frac{\partial u}{\partial r}+\frac{u}{r}+\frac{\partial w}{\partial z}\right)^2&\end{aligned}\right\}\quad(15)$$

Assuming that t and v (and consequently u) are independent of z, neglecting squares and products of small quantities, where u and w are considered small compared to v, and combining equation (15) with the three momentum equations so as to eliminate the pressure gradients, result in

$$\left.\begin{aligned}c_p\rho ur\,\frac{\partial t}{\partial r}+r\rho u\,\frac{\partial(v^2/2)}{\partial r}-k\,\frac{\partial\,(r\;\partial t/\partial r)}{\partial r}&\\ =\mu\,\frac{\partial}{\partial r}\left\{rv\left(\frac{\partial v}{\partial r}-\frac{v}{r}\right)\right\}&\end{aligned}\right\}\quad(16)$$

In laminar flow with small radial velocities, or large viscosity, equation (16) shows that $t=$ constant, that is, the static temperature is uniform because of conduction. For large radial flow or small viscosity $t+v^2/2\,c_p=$ constant, or the total temperature is uniform.

The energy equation (16) can be adapted to turbulent flow by replacing μ and k by $\rho\varepsilon$ and $\rho c_p\varepsilon_h$, respectively. The quantities ε and ε_h are the eddy diffusivities for momentum and heat transfer. Inasmuch as the assumption $\varepsilon=\varepsilon_h$ has given good results for flow through tubes, that assumption will be retained here in the absence of other experimental information. Adding a term to account for the effect of radial pressure gradient on the turbulent heat transfer, which will be discussed in the next paragraph, equation (16) becomes

$$\left.\begin{aligned}c_p\rho ur\frac{dt}{dr}+\frac{r\rho u}{2}\,\frac{dv^2}{dr}&=\\ =\frac{d}{dr}\left[r\left\{\rho c_p\varepsilon\left(\frac{dt}{dr}-\frac{1}{\rho c_p}\,\frac{dp}{dr}\right)\right\}\right]&+\\ +\frac{d}{dr}\left\{\rho\varepsilon rv\left(\frac{dv}{dr}-\frac{v}{r}\right)\right\}&\end{aligned}\right\}\quad(17)$$

As in the case of the equation of turbulent momentum, equation (17) could have been obtained by breaking the instantaneous temperatures, velocities, and densities into mean and fluctuating components and setting

$$\overline{u't'}=-\,\varepsilon(dt/dr-(1/\rho c_p)\,dp/dr)$$

and $\quad\overline{u'v'}=\quad-\,\varepsilon(dv/dr-v/r).$

The term $-(1/\rho c_p)\,dp/dr$ is added to dt/dr in equation (17) inasmuch as the turbulent heat transfer appears to be a function of pressure gradient as well as of temperature gradient. That assumption has been made by several authors [4, 7, 9]. When the turbulent particles move radially to regions of different pressure they expand or contract so that they arrive at the point of mixing at a temperature different than they would have had in a uniform pressure field. It was found in [10] that turbulent particles appear to move adiabatically except at low Peclet or Reynolds numbers, where the effect of conduction to a particle may become appreciable. Assuming the isentropic expansion or contraction of eddies, one would expect that for the case of no net heat transfer, the temperature distribution should be isentropic rather than isothermal.* That is, the relation between temperature and pressure should be given by

$$t=\text{const.}\;p^{\gamma-1/\gamma},\ \text{or}\ \frac{dt}{dr}=\frac{1}{\rho c_p}\,\frac{dp}{dr}\qquad(18)$$

which is identical to equation (17) for the case of no radial heat transfer. The addition of the term $(1/\rho c_p)\,dt/dr$ to equation (17) therefore appears to be justified. The term can also be obtained by means of a modified mixing-length theory which is given in the Appendix.

The above assumption concerning the expansion and contraction of eddies also appears to receive strong support from meteorlogical observations. An isentropic relation between temperature and pressure as altitude increases

* Although irreversible effects are operative in the fluid as a whole, it appears that the expansion or contraction of an individual eddy might be considered isentropic, inasmuch as the normal viscous stress is usually negligible in the absence of shock waves. The assumption is supported by experiment, especially by meteorological observations.

has been found for highly turbulent atmospheres, whereas for quiescent conditions the atmosphere is isothermal [11].

For small radial and axial velocities the momentum equation for the radial direction reduces approximately to

$$\frac{dp}{dr} = \frac{\rho v^2}{r} \tag{19}$$

Substituting equation (19) into (17) one finds that for large radial flows or small turbulent diffusivities the total temperature is constant as in the case of laminar flow. On the other hand, for small radial flows or large turbulent diffusivities $t - t_i = (v_i^2/2c_p r_i^2)(r^2 - r_i^2)$, in contrast to the laminar case, where the static temperature was uniform. The static temperature difference in the turbulent case is caused by the expansion and contraction of the eddies moving radially as discussed above. As in the case of the velocity distributions $\rho\varepsilon$ is considered constant.

If we divide the vortex into an annular and a core region, each with a uniform mass velocity as before, we obtain, for the core

$$\left.\begin{aligned} &\frac{\{1 - \exp(-Re_i/2\}^2}{2Re_i} r' \frac{dt'}{dr'} = \\ &= \frac{3}{Re_i r'^2}\{\exp(-Re_i r'^2/2) - 1\}^2 + \\ &+ \exp(-Re_i r'^2/2) + \\ &+ \exp(-Re_i r'^2/2)\Big[4 \ln\{\sqrt{(Re_i)}\, r'\} - \\ &- Ei\left(\frac{Re_i r'^2}{2}\right) - Ei\left(-\frac{Re_i r'^2}{2}\right) - 1{\cdot}2319\Big] \end{aligned}\right\} \tag{20}$$

where it was assumed that dt'/dr' cannot be infinite at $r' = 0$. For the annular region

$$\left.\begin{aligned} &\exp(Re_i K r'^2/2)\, r'^{1-Re_i(K-1)} \frac{dt'}{dr'} = \\ &= \left(\frac{dt'}{dr'}\right)_{r'=1} \exp(Re_i K/2) + \\ &+ \int_1^{r'} \exp(Re_i K r'^2/2)\, r'^{-Re_i(K-1)} \\ &\left[-r' \frac{d^2 v'^2}{dr'^2} + \frac{dv'^2}{dr'}\right. \\ &\left.\left\{3 - Re_i r'\left(\frac{1}{r'} - \frac{K}{r'} + Kr'\right)\right\}\right] dr' \end{aligned}\right\} \tag{21}$$

where $(dt'/dr')_{r'=1}$ is obtained from the solution for the core. Equation (21) was integrated numerically. The derivatives of v' are obtained from the solutions for the velocity equation. The quantity t' can then be obtained by numerical integration of the equation

$$t' - t_i' = \int_1^{r'} \left(\frac{dt'}{dr'}\right) dr' \tag{22}$$

In equation (20) we can see that

$$t'\{1 - \exp(-Re_i/2)\}^2/Re_i$$

is a function only of $\sqrt{(Re_i)}\, r$, so that the equation can be integrated once for all Reynolds numbers. The dimensionless total temperature difference can be obtained from the static temperature by the equation

$$T' - T_i' = t' - t_i' - 1 + v'^2.$$

Typical total and static temperature distributions are plotted in Figs. 5 and 6. The total temperature distributions are probably of more direct interest in connection with energy separation, inasmuch as the fluid will eventually be brought to rest outside the vortex; the static temperature distributions are included for comparison and also indicate the direction of heat flow by conduction. The limiting curves for zero Reynolds number

$$\{(T - T_0)/(v_0^2/2c_p) = 2\,(r/r_0)^2 - 1\}$$

and for infinite Reynolds number

$$\{(T - T_0)/(v_0^2/2c_p) = 0\}$$

are shown dashed.

The total temperature curves indicate considerable energy or temperature separation, the temperatures first rising (for large W_c/W) and then dropping as the center is approached. (For the curves where the total temperatures continuously fall as the center is approached, an overall energy balance on the vortex tube, to be discussed in the next section, indicates that the region of increasing temperatures lies between the vortex analyzed here and the tube wall.) As in the case of the velocity distributions the curves for low Re_0 and high W_c/W are somewhat similar to those for high Re_0 and low W_c/W. This is apparently due to the fact that

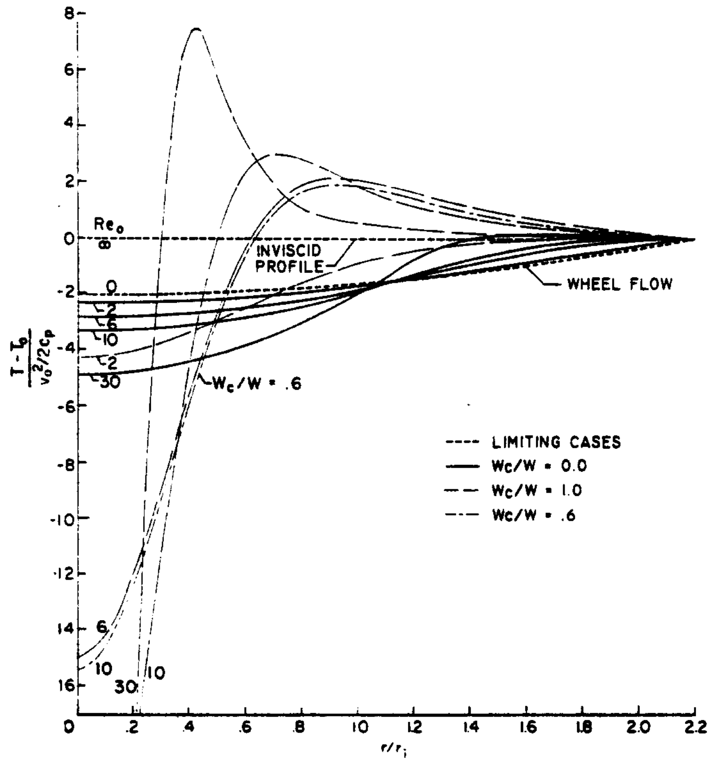

FIG. 5. Total temperature distributions in turbulent vortex. $r_0/r_i = 2{\cdot}2$.

the flow out of the core region, which seems to control the shape of the curves, tends to be the same in both cases. The static temperature curves indicate that in all cases the heat conduction due to temperature gradients is toward the center of the vortex. Thus the cooling at the center cannot be caused by conduction due to temperature gradients; it may be caused by the expansion and contraction of the turbulent eddies or by viscous shear. The causes of the energy separation will be considered in detail in a later section.

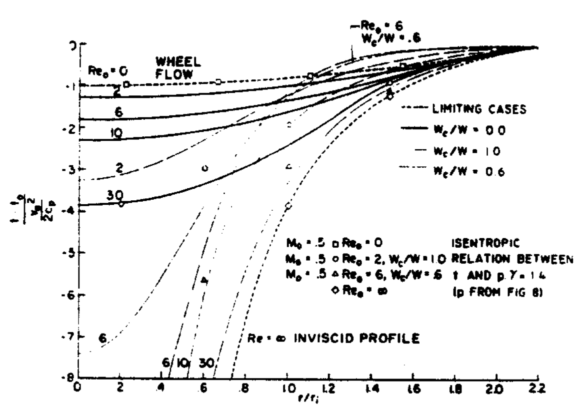

FIG. 6. Static temperature distributions in turbulent vortex. $r_0/r_i = 2{\cdot}2$.

For purposes of comparison with the predicted static temperature distributions in a vortex, temperatures obtained for an isentropic relation between static temperature and pressure (pressures from Fig. 8) are plotted as points in Fig. 6. For small radial flows the temperatures are in approximate isentropic equilibrium with the pressures because of expansion and contraction of eddies. For larger radial flows the deviation of the vortex temperatures from the equilibrium temperatures increases. For very high radial-flow Reynolds numbers the distributions are again isentropic. However, there is no total temperature separation in that case. The same result is obtained for laminar flow.

To check the temperature results against experiment we again use the experimental data of [7]. The same assumptions as were used in comparing the velocity results are used here. The comparison is shown in Fig. 7. The shapes of the analytical and experimental curves agree reasonably well, indicating lower turbulent Reynolds numbers than were indicated for the velocity profiles. As was mentioned in connection with the velocity profiles, the indicated turbulent Reynolds numbers there might be too high because of boundary layer effects near the tube wall.

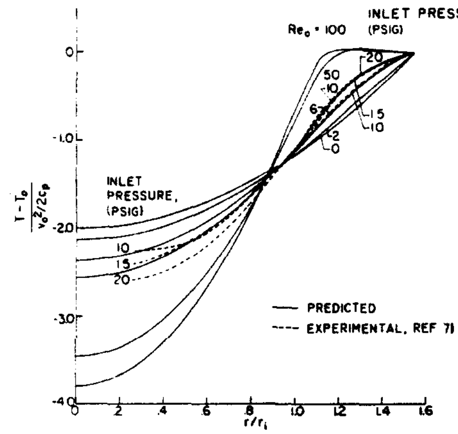

FIG. 7. Comparison of analytical total temperature profiles with experiments in [7]. $W_e/W = 0$, $r_0/r_i = 1{\cdot}54$.

Turbulent Reynolds number

Thus far the turbulent Reynolds number Re_0 has been considered as a free parameter in the analysis, and no attempt has been made to predict its value. The unknown quantity in that parameter is, of course, the eddy diffusivity or eddy viscosity. It is of interest to attempt to predict the eddy diffusivity by using von Kármán's similarity hypothesis, which has been successful for flow through tubes. The expression will first be modified for circular flow as follows: For purposes of analysis it is assumed that the turbulence at a point is dependent only on the shearing deformation at the point and in the vicinity of the point; that is, it is a function of the deformation and its derivatives. If we exclude derivatives higher than the first, then $\varepsilon = f\{(dv/dr - v/r), d/dr(dv/dr - v/r)\}$. Application of dimensional analysis then gives

$$\varepsilon = \frac{-\kappa^2 (dv/dr - v/r)^3}{[d/dr\ (dv/dr - v/r)]^2} \tag{23}$$

The derivation for equation (23) can also be used to obtain the usual Kármán expression for the case of rectilinear flow. For the outer portion of the vortex, except at the lowest Reynolds numbers, the tangential velocity is given approximately by $v = v_0 r_0/r$. The expression for ε at the outer edge of the vortex then becomes

$$\epsilon = \kappa^2 v_0 r_0/2, \text{ or}$$

$$Re_0 = -\frac{2}{\kappa^2}\frac{u_0}{v_0} \tag{24}$$

In the present analysis it is assumed that Re_0 is uniform ($\rho\varepsilon$ = constant), so that equation (24) is applied throughout the vortex. For flow through a tube or channel, κ has been found to lie between 0·3 and 0·4. If we take $\kappa = 0{\cdot}3$, then for the experiments in [7], the following values of Re_0 are calculated from equation (24): For inlet pressure $p = 10$ lb/in² gauge, $Re_0 = 6{\cdot}9$, for $p = 15$, $Re_0 = 6{\cdot}7$. and for $p = 20$, $Re_0 = 7{\cdot}1$. Comparison of these values with those indicated by the experimental and analytical temperature distributions in Fig. 7 indicates reasonable agreement. However, more work should be done to prove or disprove the general validity of equations (23) or (24). It appears that in some cases the turbulence in the vortex might be influenced by the presence of the tangential nozzles in the wall.

Pressure distributions

In order to obtain an idea of the pumping power required to force the fluid through the vortex, the pressure distribution in the vortex is required. Both the static and total pressures will be calculated, inasmuch as part of the rotational kinetic energy leaving the vortex can probably be recovered. To calculate the static pressure distributions we use equation (19) and the perfect gas law to obtain

$$\frac{p}{p_0} = \exp\left[\frac{2\gamma}{\gamma - 1} \times \int_{r_i}^{r'} \frac{(v/v_0)^2\, dr'}{r'\{(t - t_0)/(v_0^2/2c_p) + 2/(\gamma - 1)M_0^2\}}\right] \tag{25}$$

Thus in order to plot the pressure distributions the parameters M_0 and γ, in addition to those required for the velocity and temperature distributions, must be used. Total pressure distributions can be obtained from the static pressure distributions by the relation

$$\frac{P}{P_0} = \frac{p}{p_0} \times \left[\frac{1 + \{(v/v_0)^2/[(t-t_0)/(v_0^2/2c_p) + 2/\{(\gamma-1)M_0^2\}]\}}{1 + \{(\gamma - 1)/2\}M_0^2}\right]^{\gamma/(\gamma-1)} \tag{26}$$

Note that for these equations to apply the quantity $t - t_0/(v_0^2/2c_p) + 2/(\gamma - 1)M_0^2$ must be greater than zero, inasmuch as the pressure (and temperature) will go to zero as that quantity approaches zero.

Static and total pressure distributions for some typical cases are plotted in Figs. 8 and 9. For $Re_0 = \infty$ the total pressure is uniform, inasmuch as the flow is inviscid for that case, although the static pressure drops sharply as the center is approached. However, for realistic Reynolds numbers the differences between the static and total pressure curves are not nearly as great.

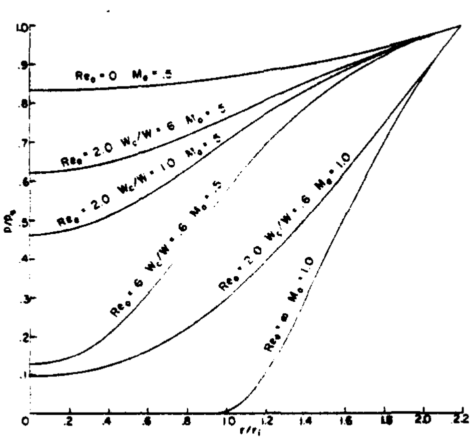

FIG. 8. Static pressure distributions in turbulent vortex. $r_0/r_i = 2{\cdot}2$, $\gamma = 1{\cdot}4$.

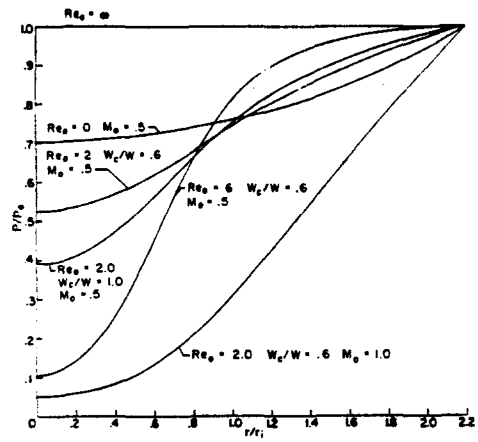

FIG. 9. Total pressure distributions in turbulent vortex. $r_0/r_i = 2{\cdot}2$, $\gamma = 1{\cdot}4$.

The curves for $Re_0 = 2$ and $M_0 = 1{\cdot}0$ correspond approximately to Hilsch's vortex tube data for inlet to outlet pressure ratios of 6 and 10 (Fig. 10). (Hilsch's data will be discussed in the next section.) It is difficult to compare the pressures in the vortex with those measured by Hilsch outside the vortex because of uncertainty in the losses between the vortex and the environment. However, the pressure distribution curves in Fig. 8 and 9 indicate both static and total pressure ratios between the outer radius and some average radius in the core of the same order of magnitude as the pressure ratios obtained by Hilsch. (Inlet pressure in atmospheres on Fig. 10 is equivalent to pressure ratio between inlet and outlet.)

Ranque–Hilsch tube

In comparing the analytical results with experimental results obtained in actual vortex tubes, one cannot consider the containing tube to be coincident with the outer radius of the vortex which has been analyzed. The velocity at the tube wall is zero, whereas that at the outer radius of the vortex is finite. Also, the heat conducted through the tube wall can be neglected, whereas that conducted across the outer radius of the vortex is not negligible. In addition, the presence of tangential nozzles in the wall for the entering fluid will tend to destroy the axial symmetry of the flow near the wall. It is therefore assumed that there is a region of fluid between the outer radius of the vortex and the tube in which there is no axial flow. The flow in this region will be complicated and no attempt will be made to analyze it in detail. However, the difference between the total temperature of the fluid entering the tube through the tangential nozzles and the temperature at the outer radius can be obtained from an overall energy balance on the system as

$$T_e - T_0 = (W_c/W)(T_c - T_0) + \\ + (1 - W_c/W)(T_h - T_0)$$

where the specific heat is assumed uniform and the tube is adiabatic. The temperature T_e in general differs from the total temperature at the outer radius of the vortex. The temperatures T_c and T_h are the integrated mixed mean temperatures of the fluid leaving the system axially from the core and from the annulus of the vortex and are obtained from the total temperature distributions and the following equations:

$$T_c - T_0 = 2\int_0^1 (T - T_0)r'dr' \quad (27)$$

and

$$T_h - T_0 = \frac{2\int_1^{r_0/r_i} (T - T_0)r'dr'}{(r_0/r_i)^2 - 1} \quad (28)$$

Predicted values of $(T_h - T_e)/(v_0^2/2c_p)$ and $(T_c - T_e)/(v_0^2/2c_p)$ are plotted in Fig. 10 as functions of the ratio of axial mass flow through the core to total mass flow and turbulent Reynolds number for a radius ratio of 2·2. The upper and lower sets of curves are related by the overall energy balance

$$\frac{W_c}{W}(T_c - T_e) + \left(1 - \frac{W_c}{W}\right)(T_h - T_e) = 0 \quad (29)$$

The limiting curves for $Re_0 = 0$ are given by

$$(T_h - T_e)/(v_0^2/2c_p) = W_c/W$$

and

$$(T_c - T_e)/(v_0^2/2c_p) = (W_c/W) - 1$$

For $Re_0 = \infty$ and $W_c/W > 0$,

$$T_h - T_e = T_c - T_e = 0$$

The curves indicate that the total temperature separation between the two streams emerging from the vortex increases as the turbulent radial flow Reynolds number Re_0 increases, but that the value of W_c/W for maximum temperature depression approaches zero for large Re_0.* For very large values of Re_0 no total temperature separation will occur between the hot and cold streams except for values of W_c/W essentially equal to zero. This result indicates why turbulent rather than laminar flow is necessary to explain the energy separation in actual vortex tubes. (The curves for turbulent flow are qualitatively similar to those for laminar flow when $\rho\varepsilon$ in the Reynolds number is replaced by μ.) The laminar Reynolds numbers in vortex tubes are several orders of magnitude higher than the values of Re_0 shown in Fig. 10. Thus if the vortex is laminar, the effective Reynolds number will be so high that essentially no energy separation can take place.

For a given Reynolds number the curves indicate that the energy separation could be increased by increasing the tangential velocity v_0 or by decreasing c_p. The optimum value of Re_0 for favorable energy separation for a range of values of W_c/W appears to be about 6. Comparison with the velocity distribution curves in Fig. 2 indicates that the velocity gradients and viscous shear are reasonably large throughout the vortex for a Reynolds number of 6. As will be seen later, the energy separation is related to the viscous shear. The viscous shear is also large for much larger Reynolds numbers, but for those Reynolds numbers the fluid does not remain in the vortex long enough for appreciable energy separation to take place (except very close to the center).

Note that in general low total temperatures in the cold stream are obtained at low values of W_c/W, whereas high temperatures in the hot stream are more readily obtained at large values of W_c/W.

Experimental data obtained by Hilsch [1] are plotted in Fig. 10 as dashed lines. His apparatus consisted of a tube with a nozzle

* The difference between the appearance of these curves and corresponding curves in [5] is due to the fact that the Reynolds number in [5] was based on the inside rather than on the outside radius.

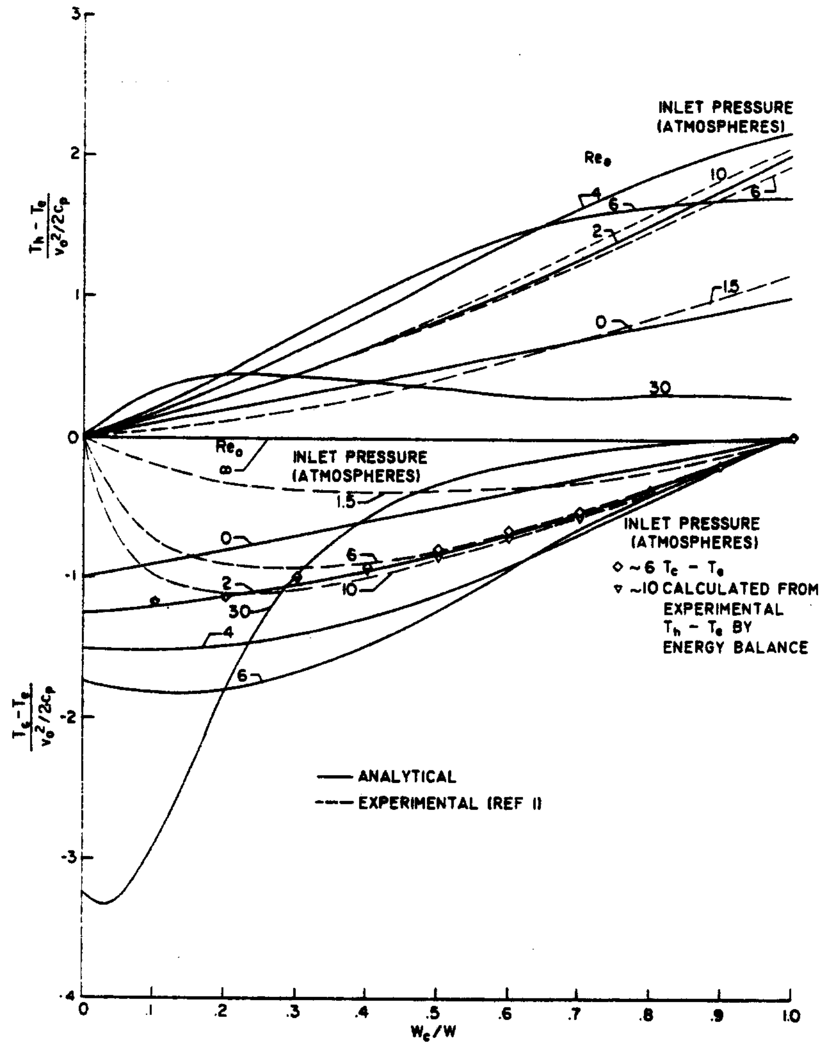

FIG. 10. Predicted overall energy separation for turbulent vortex tube and comparison with experiments in [1]. $r_0/r_i = 2{\cdot}2$.

through which air could enter tangentially so as to form a vortex within the tube. Hot air could then be withdrawn through an annular valve at one end of the tube and cold air through an orifice at the other end. The entrance nozzle was near the end of the tube where the orifice was located. In comparing the analytical and experimental results it was assumed that the air entered the tube at Mach 1, inasmuch as the mass flow was independent of the exit valve setting for a given inlet pressure. The experimental curves for various inlet pressures shown in Fig. 10 should therefore correspond to our curves for various $Re_0 \equiv \rho_0 u_0 r_0/\rho\varepsilon$ if it is assumed that $\rho\varepsilon$ is a function only of entering conditions and is thus independent of W_c/W. The radius ratio in the analysis was taken as 2·2, corresponding to the ratio of the tube to orifice radius in the experiment.

Good agreement is indicated between the analytical curve for $Re_0 = 2$ and the experimental curves for inlet pressures of 6 and 10 atm except at the lower values of W_c/W. However, if we calculate the cold-stream temperatures from the experimental hot-stream temperatures and the energy balance equation (equation (29)), the results agree closely with the analytical curve for all values of W_c/W. Thus, the experimental cold-stream temperatures are probably too high because of thermal conduction radially along the tube end wall or from the atmosphere to the stream. This possibility was mentioned by Hilsch. The fact that the curve for an inlet pressure of 1·5 atm (low flow rate) lies above the curve for $Re_0 = 0$ can probably also be explained by external conduction.

In order to study the effect of radius ratio, curves for total temperature separation at various radius ratios are plotted in Fig. 11 for a

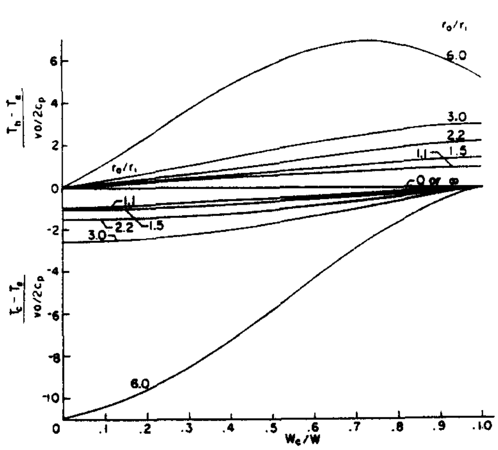

FIG. 11. Effect of radius ratio on overall energy separation for turbulent vortex tube. $Re_0 = 4·0$.

Reynolds number of 4. A considerable increase in temperature separation is indicated as the radius ratio increases from 1·1 to 6. This is apparently due to the fact that the total temperature drops as the vortex center is approached (Fig. 5). A narrow cold stream will therefore have a lower average total temperature than a wider one.

CAUSES OF THE TOTAL TEMPERATURE SEPARATION

Although a considerable amount of discussion exists in the literature concerning the causes of the temperature separation in the vortex tube, no general agreement seems to have been reached. In the present section the causes of the separation are studied by examining the magnitudes of the various terms in the energy equation.

In order to determine whether compressibility in a fluid is necessary for temperature separation to occur, the incompressible case will first be considered. For this case it is convenient to consider static, rather than total temperatures, inasmuch as the total or stagnation temperature depends on the process by which the fluid is brought to rest. If the fluid is brought to rest isentropically, the total and static temperatures will be equal. In other cases the total temperature will be higher because of friction.

For an incompressible fluid the static temperature change of a fluid element depends only on the heat added to the element by conduction and by dissipation. The energy equation thus can be written as

$$\rho c_v \frac{Dt}{D\theta} = \rho c_v \varepsilon \frac{1}{r} \frac{d}{dr}\left(r \frac{dt}{dr}\right) + \phi \qquad (30)$$

where the first term is the rate of change of internal energy per unit volume of the element, the second term is the rate at which heat is being transferred into the element by turbulent conduction, and the last term is the dissipation. If it is assumed that the rate of production of turbulent energy at a point equals the rate of turbulent dissipation, the expression for ϕ can be written as $\phi = \rho\varepsilon(dv/dr - v/r)^2$. In dimensionless form the energy equation becomes

$$\frac{Dt'}{D\theta'} = \frac{1}{Re_i r'} \frac{d}{dr'}\left(r' \frac{dt'}{dr'}\right) + \frac{2}{Re_i}\left(\frac{dv'}{dr'} - \frac{v'}{r'}\right)^2 \qquad (31)$$

The terms in the incompressible energy equation are plotted in Fig. 12 for the case of uniform axial flow. As a fluid element moves toward the center the dissipation term tends to increase the temperature of the particle, as would be expected. Because of the higher temperatures near the center, the center portion then tends to lose heat by conduction and the outer regions gain heat. However, the net result (shown dashed) is that the particle continuously increases in static temperature as it spirals inward toward the center.

The total temperature at any radius will never be lower than the static temperature, as discussed earlier. Therefore for an incompressible fluid there appears to be no possibility of obtaining an energy separation in which the total temperature at the center of the vortex is lower than the entering temperature.

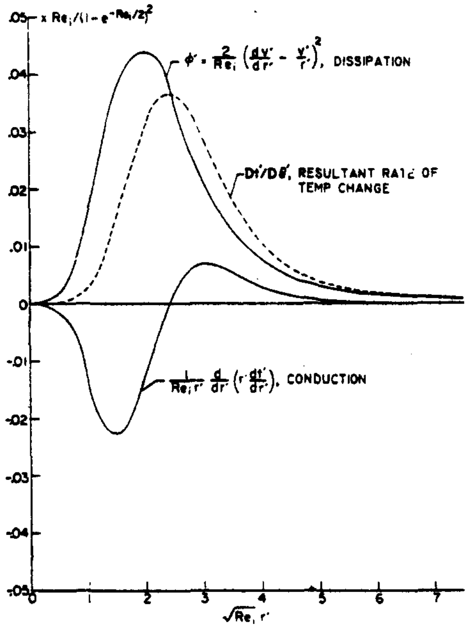

FIG. 12. Terms in incompressible energy equation (equation (31)) contributing to rate of change of temperature of fluid element with respect to time. Uniform axial mass velocity.

Thus the first requirement for energy separation to take place in a vortex is that the fluid be compressible. It should be remembered, however, that the expansion of a compressible fluid does not always produce a cooling of the fluid. As is well known, the expansion of a perfect gas flowing through an adiabatic tube or nozzle does not result in a total temperature drop. In order for cooling to take place, it is necessary that the fluid do work while it expands, as in a turbine, or that heat be transferred out of the fluid. Similarly, for the total temperature increase, work would have to be done on the fluid, or heat transferred into it. In order to see how these observations apply to the vortex, we rewrite the energy equation for a perfect gas (equation 17)):

$$\rho c_p \frac{D}{D\theta}\left(t + \frac{v^2}{2c_p}\right) = \frac{1}{r}\frac{d}{dr}\left(r\rho c_p \varepsilon \frac{dt}{dr}\right) - \\ - \frac{1}{r}\frac{d}{dr}\left(\frac{r\rho\varepsilon}{\rho}\frac{dp}{dr}\right) + \frac{1}{r}\frac{d}{dr}(rv\tau) \quad (32)$$

The left side of this equation can be written as $\rho c_p\, DT/D\theta$. Equation (32) shows that the rate of change of total temperature of a fluid element as it spirals toward the center depends on the following contributions:

$\frac{1}{r}\frac{d}{dr}\left(r\rho c_p\varepsilon\frac{dt}{dr}\right)$,	turbulent heat transfer into fluid element by temperature gradients;
$-\frac{1}{r}\frac{d}{dr}\left(\frac{r\rho\varepsilon}{\rho}\frac{dp}{dr}\right)$,	turbulent heat transfer into fluid element by pressure gradients (by expansion and contraction of eddies);
$\frac{1}{r}\frac{d}{dr}(rv\tau)$,	turbulent shear work done on element.

Equation (32) can be written in dimensionless form as

$$\frac{\rho}{\rho_i}\frac{DT'}{D\theta'} = \frac{1}{Re_i r'}\frac{d}{dr'}\left(r'\frac{dt'}{dr'}\right) - \frac{2}{Re_i r'}\frac{dv'^2}{dr'} + \\ + \frac{2}{Re_i r'}\frac{d}{dr'}\left\{r'v'\left(\frac{dv'}{dr'} - \frac{v'}{r'}\right)\right\} \quad (33)$$

where equation (19) was used for $(1/\rho)dp/dr$, and the turbulent shear stress τ was set equal to $\rho\varepsilon(dv/dr - v/r)$.

In order to illustrate the magnitudes of the contributions to the rate of change of total temperature of a particle we again consider the case of uniform axial flow. Other axial flow distributions should give qualitatively similar results. The various contributions are plotted in Fig. 13. Although the terms for turbulent conduction due to temperature gradients and to pressure gradients are individually very large, especially near the vortex center, they tend to cancel. That is, the conduction of heat into the core region by temperature gradients is about equal to the heat conducted out by pressure gradients, or by expansion and contraction of eddies. Thus the shear work term produces most of the energy separation. This is indicated by the fact that the curve for the sum of the contributions to the total temperature change (shown dashed) follows fairly closely the contribution due to shear work. Although the net conduction effect on $dT/d\theta$ is reasonably small, it is negligible

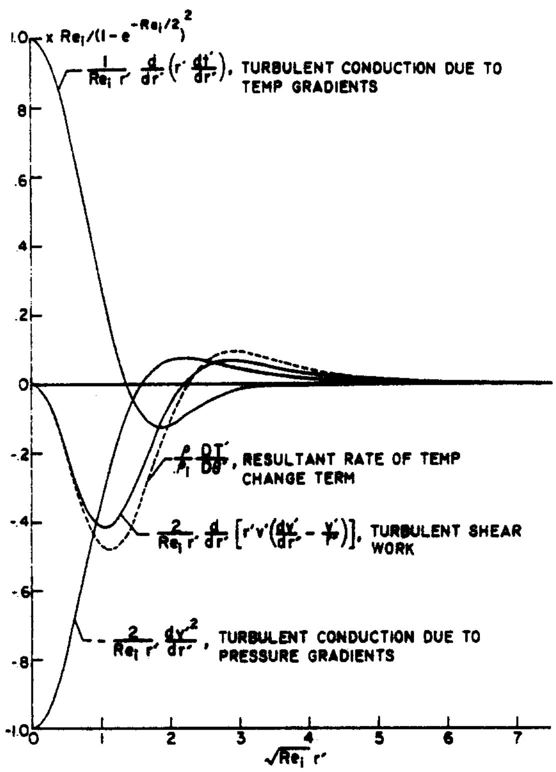

FIG. 13. Terms in compressible energy equation (equation (33)) contributing to rate of change of total temperature of fluid element with time. Uniform axial mass velocity.

only for very small radii or radial flow Reynolds numbers. More will be said about this limiting case later. At very large radii the shear work done on a fluid element is essentially zero because of the small tangential velocities and velocity gradients in that region. At slightly smaller radii the shear work becomes positive and the total temperature of a fluid element increases with time. At still smaller radii the shear becomes negative and the total temperature of an element decreases with time. Comparison of these curves with the tangential velocity profile curve in Fig. 3 indicates that the region of positive shear work or of increasing total temperature corresponds to the region in which the velocity profile is still essentially inviscid ($v \propto r^{-1}$). Then as the fluid element moves to smaller radii the viscous or turbulence effects cause the velocity profile to depart from the $1/r$ variation. In that region the shear work done on the element becomes negative due to the slowing-down tendency of the turbulent viscosity, and the total temperature drops. Thus the energy separation is dependent on the tangential velocity profile. The overall result is that the fluid in the core region does shear work on the fluid in the outer region as it expands while traveling toward the center. Thus energy is transferred from the core region to the annular region with a resultant total temperature separation. A smaller additional energy transfer is effected by the expansion and contraction of eddies in a radial pressure gradient.

Inasmuch as the shear work term in the compressible energy equation gives the most important contribution to the change in total temperature of a fluid element as it moves radially, it is instructive to determine the contributions of various other physical processes to that term. This can be done by multiplying the momentum equation (2) by v and combining with the other momentum equation (19) to give

$$\frac{1}{r}\frac{d}{dr}(rv\tau) = \rho\varepsilon\left(\frac{dv}{dr} - \frac{v}{r}\right)^2 + \\ + \rho u\left[\frac{d(v^2/2)}{dr} + \frac{1}{\rho}\frac{dp}{dr}\right] \quad (34)$$

That is, the shear work is distributed between a dissipation term, a kinetic energy term and a potential or pressure energy term. In the region where the shear work term and $DT/d\theta$ are positive, the velocity distribution is approximately that for inviscid flow ($v \propto r^{-1}$). Thus the kinetic and potential energy terms nearly cancel (substitute equation (19) for dp/dr), so that the important contribution to the shear work in that region is the dissipation. The increase in total temperature with time of a fluid element in the annular region is therefore due principally to viscous (or turbulent) dissipation. The dissipation can be important in a region where the velocity profile is approximately that for inviscid flow because the shear stresses on the sides of a fluid element, although individually large, nearly cancel. Thus the shear stress can have a negligible effect on the velocity profile and still produce significant dissipation.

In the region near the center, where the shear work and $DT/d\theta$ are negative, wheel flow is approached, and the dissipation becomes less important. The important contributions to the negative shear work, and thus to the drop in total temperature of a fluid element in that region are then the kinetic and the potential or pressure energy terms, both of which are negative. For wheel flow the two terms are equal.

For the special case of no radial flow ($Re_0 = 0$) Fig. 13 apparently yields no pertinent information; for that case $DT/d\theta$ for a fluid particle is zero. Nevertheless the total temperature at the center of such a vortex is lower than that in the outer region (Fig. 5). In that case we can consider the total temperature separation to take place somewhat as follows: For purposes of discussion we first neglect conduction due to expansion and contraction of eddies. The static temperature will then tend to be uniform, inasmuch as conduction due to temperature gradients will iron out any temperature differences (no external heat transfer). Also, for no radial flow the fluid rotates as a solid body ($v \propto r$). Thus since the static temperature is uniform, the total temperature will be lower near the center because of the lower velocities there. If turbulence occurs in the vortex, the total temperature near the center will be lowered still more because of heat conducted toward the outer regions by expansion and contraction of eddies in a pressure gradient.

If the radial flow is not zero but very small, the above picture will still apply, inasmuch as the very small radial flow should not alter the velocity and temperature distributions appreciably. In this case we could, of course, also consider the cooling of a fluid element as being due to the shear work as discussed earlier in connection with Fig. 13. The two ways of looking at the energy separation are closely related, inasmuch as the shear work can be divided into a kinetic energy term and a pressure gradient term (equation (34)) the dissipation term drops out for wheel flow). The pressure gradient in turn is related to the temperature gradient by equation (18). Thus the drop in total temperature of a fluid element as it moves slowly toward the center can be thought of as being due either to the shear work done by the particle or to the lower velocities and static temperatures of the fluid near the center. The static temperatures are lower near the center because of the heat transferred to larger radii by pressure gradients.

It should be noticed that, although a long tube extending considerably beyond the location of the tangential nozzles for the entering fluid is usually used in investigations of energy separation, the present model makes no mention of such a tube. The energy separation is assumed to take place entirely within the vortex where the tangential nozzles are located. This is in agreement with the experiments in [7], where the greatest energy separation was found to take place in the tube cross-section near the tangential nozzles. In addition, some recent experiments by Savino and Ragsdale [13] indicate that considerable energy separation can take place in a vortex contained between two flat disks without an attached tube. The flow emerged from an opening at the center with a diameter on the order of the plate spacing. Most of the energy separation took place near the opening.

The energy separation in vortex tubes is sometimes attributed to unsteady effects (other than the turbulence effects considered here). Although such effects might augment the energy separation under certain conditions, the present analysis indicates that considerable separation can be accounted for by considering only steady-state effects.

CONCLUSIONS

The analysis indicated that the dimensionless tangential velocity and temperature distributions are functions of the following parameters: The ratio of axial flow out of the core of the vortex to the total mass flow, the ratio of the core radius to the radius of the vortex, and a turbulent radial-flow Reynolds number which contains the eddy viscosity rather than the molecular viscosity. For the pressure distributions it was necessary in addition to specify the Mach number at a given radius and the ratio of the heat capacities.

The importance of turbulence for energy separation was found to be twofold: First, it causes the effective Reynolds number to remain low (where energy separation can take place), even when the laminar Reynolds number is high. This is because the turbulent viscosity may be several orders of magnitude higher than the molecular viscosity. (However, it would not pay to increase the turbulence level indefinitely, inasmuch as an optimum turbulent Reynolds number was obtained.) Secondly, there is an additional energy separation in the turbulent case due to the expansion and contraction of the eddies as they move radially in a pressure gradient. The predicted curves for velocity and temperature distributions, as well as for overall energy separation, closely resembled experimental curves, so that it appears that the model analyzed displays most of the features of actual vortex tubes.

In analyzing the causes of the energy separation it was determined first that the fluid must be compressible, since the total temperature of a particle in an incompressible vortex can only increase, owing to the dissipation. By considering the magnitudes of the terms in the compressible energy equation, it was found that the terms for turbulent conduction due to temperature gradients and to pressure gradients, although individually large, tended to cancel. Thus most of the total temperature change of a fluid element as it spiraled toward the center was due to the shear work done on the element (positive in the outer region, negative in the core). Therefore the energy separation depends on the tangential velocity profile, in particular, on the deviation of the profile near the center from that for inviscid flow. The overall effect is that the fluid in the core region does shear work on the fluid in the outer region with a resultant total temperature separation. The shear work term was further divided into a dissipation term, a kinetic energy term and a potential or pressure energy term. In the region of high total temperatures the dissipation term was found to produce most of the heating of a fluid element. The decrease of total temperature of an element as it moves in the core region was due principally to the kinetic and pressure energy terms, both of which are negative in that region.

APPENDIX

Derivation of Pressure Gradient Conduction Term by Modified Mixing-length Theory

Although the mixing-length theory may be an oversimplification of the actual turbulent transfer in a vortex, it provides a convenient way of arriving at the pressure gradient conduction term in equation (17). In the following analysis. eddies are assumed to move transversely in the vortex between cylindrical surfaces (1) and (2) which are separated by the small distance l, the average mixing length at a particular radius.

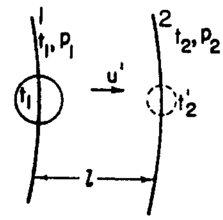

Eddies also move axially and tangentially, but these should not affect the radial heat transfer. The eddies originate from an instability at either surface (1) or (2) and travel to the other surface where they mix with the fluid. Consider an eddy of fluid which originates at the inner surface (1), where it has the time average temperature and pressure of the fluid at surface (1). As discussed in the body of the text the eddy is assumed to be compressed isentropically as it moves to the region of higher pressure at (2). As the eddy arrives at surface (2), conservation of mass requires that an equal mass of fluid must leave. The net heat transported to surface (2) is then equal to the mass of the eddy multiplied by $c_p(t_2' - t_2)$, where t_2' is the temperature of the eddy as it arrives at surface (2) and t_2 is the temperature of the surrounding fluid. The turbulent heat transfer per unit area per unit time from surface (1) to surface (2) is then given by

$$q_t = c_p \rho f u'(t_2' - t_2) \tag{A1}$$

where f is the fraction of surface (2) on which eddies are arriving, and u' is the average velocity of the eddies. Equation (A1) can be written as

$$q_t = - c_p \rho f u' l \left(\frac{\Delta t_f}{l} - \frac{\Delta t_e}{l}\right) \tag{A2}$$

where Δt_f is the change in average fluid temperature between (1) and (2) and Δt_e is the corresponding change in eddy temperature. In differential form equation (A2) becomes

$$q_t = -c_p \rho f u' l \left(\frac{dt}{dr} - \frac{dt_e}{dr} \right)$$

For an isentropic compression equation (18) can be substituted to give

$$q_t = -c_p \rho \varepsilon \left(\frac{dt}{dr} - \frac{1}{\rho c_p} \frac{dp}{dr} \right) \qquad \text{(A3)}$$

where the eddy diffusivity ε was substituted for $fu'l$. This expression for turbulent heat transfer is the same as the expression for turbulent heat transfer in equation (17).

REFERENCES

1. R. Hilsch, *Rev. Sci. Instrum.* **18**, (1947).
2. R. Westley, *A Bibliography and Survey of the Vortex Tube*. The College of Aeronautics, Cranfield (1954).
3. C. D. Pengelley, *Flow in a Viscous Vortex*. Report 494C-1, TN 56-126, Southwest Research Institute (1956).
4. J. J. Van Deemter, *Appl. Sci. Res.* A 3, 3 (1952).
5. R. G. Deissler and M. Perlmutter, *An Analysis of the Energy Separation in Laminar and Turbulent Compressible Vortex Flows*. Heat Transfer and Fluid Mechanics Institute, Stanford University Press (1958).
6. H. A. Einstein and H. Li, *Steady Vortex Flow in a Real Fluid*. Heat Transfer and Fluid Mechanics Institute, Stanford University Press (1951).
7. J. P. Hartnett and E. R. G. Eckert, *Experimental Study of the Velocity and Temperature Distribution in a High Velocity Vortex Type Flow*. Heat Transfer and Fluid Mechanics Institute, Stanford University Press (1956).
8. S. Pai, *Viscous Flow Theory*, pp. 37, 43. Van Nostrand, New York (1956).
9. R. Kassner and E. Knoernschild, *Friction Laws and Energy Transfer in Circular Flow*. TR No. F-TR2198-ND, WADC (1948).
10. R. G. Deissler, *Analysis of Fully Developed Turbulent Heat Transfer at Low Peclet Numbers in Smooth Tubes with Applications to Liquid Metals*. NACA RM E52F05 (1952).
11. *Meteorology and Atomic Energy* p. 27. Supt. Docs., U.S. GPO, Wash., D.C. (1955).
12. J. E. Lay, *Trans. Amer. Soc. Mech. Engrs.* 202 (1959).
13. J. M. Savino and R. T. Ragsdale, *Some Temperature and Pressure Measurements in Confined Vortex Fields*. ASME Preprint No. 60-SA-4 (1960).